RESEARCH PAPER

FORMULATION AND DEVELOPMENT OF CURCUMIN-LOADED NANOBUBBLES: PHYSICOCHEMICAL CHARACTERISATION AND IN VITRO RELEASE EVALUATION

Solanki S[1], Kamble S[1], Bankar SD[1], Solanki N[1]*, Jadhav S[2], Posa MK[3], Khan SKS[4], Goswami H[5], Dubey V[6], Damerla S[7], Kumari S[8]

[1]Department of Pharmaceutics, HSBPVT's GOI Faculty of Pharmacy, Kashti, Ahilyanagar, Maharashtra, India
[2]Bharati Vidyapeeth's College of Engineering for Women, Pune - 411043, Maharashtra, India
[3]Department of Pharmaceutical Technology, School of Health and Medical Sciences, Adamas University, Barasat, Kolkata - 700126, West Bengal, India
[4]Department of Pharmaceutical Analysis, School of Pharmacy, Dhanalakshmi Srinivasan University, Samayapuram, Trichy - 621112, Tamil Nadu, India
[5]Raj Kumar Goel Institute of Technology (Pharmacy), Ghaziabad, Uttar Pradesh - 201013, India
[6]Bharati Vidyapeeth (Deemed to be University) College of Ayurved, Pune, Maharashtra, India
[7]BGS Global Institute of Pharmaceutical Sciences, Kengeri, Bengaluru, Karnataka, India
[8]Sarala Birla University, Ranchi, Jharkhand, India

Corresponding author**
Solanki N
[1]Department of Pharmaceutics, HSBPVT's GOI Faculty of Pharmacy, Kashti, Ahilyanagar, Maharashtra, India
E-mail: drnikunjsolanki@gmail.com

Received: 25 June 2026 | Revised: 01 July 2026 | Accepted: 06Aug 2026 | Available Online: 08Aug 2026

ABSTRACT

Curcumin possesses wide pharmacological potential, but its very low aqueous solubility and poor dispersion limit formulation development. The present study aimed to formulate curcumin-loaded nanobubbles using a phospholipid-polymer shell and to evaluate their physicochemical characteristics, solid-state behaviour and in vitro release at pH 7.4. Curcumin-loaded nanobubbles were prepared using Epikuron 200, chitosan, palmitic acid, Pluronic F68 and sulfur hexafluoride. Preliminary processing and formulation variables were screened, and the selected composition was prepared by gradual addition of an ethanolic lipid phase to an aqueous chitosan-Pluronic F68 phase, followed by solvent evaporation, probe sonication and sulfur hexafluoride purging. The selected formulation contained curcumin 10 mg, Epikuron 200 121 mg, chitosan 0.22% w/v, palmitic acid 20 mg and Pluronic F68 0.28% w/v in 10 mL. It showed a particle size of 361.8 ± 4.6 nm, PDI of 0.286 ± 0.009, zeta potential of +28.0 ± 0.7 mV, entrapment efficiency of 77.7 ± 0.9% and drug loading of 4.67 ± 0.03%. FTIR spectra showed retention of characteristic curcumin bands without formation of unexplained new peaks. Comparative DSC and PXRD patterns indicated reduced crystalline order of curcumin after formulation. At pH 7.4, cumulative curcumin release at 24 h increased from 60.85 ± 0.54% without ultrasound to 83.56 ± 0.34% after ultrasound exposure. The release profiles were best described by the Korsmeyer-Peppas model. The developed nanobubbles provided satisfactory physicochemical properties and ultrasound-enhanced curcumin release at pH 7.4.

Keywords: Curcumin; nanobubbles; chitosan; sulfur hexafluoride; solid-state characterisation; ultrasound-responsive release

How to cite this article: Solanki S, Kamble S, Bankar SD, Solanki N, Jadhav S, Posa MK, Khan SKS, Goswami H, Dubey V, Damerla S, Kumari S. Formulation and development of curcumin-loaded nanobubbles: physicochemical characterisation and in vitro release evaluation. Int J Drug Deliv Technol. 2026;16(74s): 1674-1684. DOI: 10.25258/ijddt.16.74s.138

INTRODUCTION

Curcumin is a naturally occurring polyphenolic compound obtained from Curcuma longa. It has been investigated for antioxidant, anti-inflammatory and anticancer effects; however, its pharmaceutical application is restricted by poor aqueous solubility, limited dissolution, instability and rapid metabolism.[1,2]

Nanobubbles are submicrometre gas-containing carriers surrounded by lipid, polymeric, protein or

hybrid shells. Their small dimensions, high interfacial area and response to an acoustic field make them useful for improving drug dispersion and for externally triggered release.[3,4,5]

In the present formulation, Epikuron 200 was selected as a phospholipid shell-forming material, chitosan as a cationic polymer, palmitic acid as a hydrophobic co-lipid and Pluronic F68 as a steric stabiliser. Sulfur hexafluoride was selected as the gaseous phase because of its low aqueous solubility and use in gas-filled carrier systems.[3,6]

The objective of the present study was to formulate and develop curcumin-loaded nanobubbles, identify suitable processing and composition ranges, characterise the selected formulation and evaluate its in vitro release at pH 7.4 with and without ultrasound exposure. The biological anticancer evaluation was intentionally not included in this paper.

MATERIALS AND METHODS

Materials

Curcumin and palmitic acid were obtained from Loba Chemie Pvt. Ltd., Mumbai, India. Epikuron 200 was supplied by Cargill Deutschland GmbH, Germany. Low-molecular-weight chitosan was obtained from HiMedia Laboratories Pvt. Ltd., Mumbai, India, and Pluronic F68 was obtained from BASF, Germany. Sulfur hexafluoride was obtained from an authorised specialty-gas supplier. All other reagents and solvents were of analytical grade.

Preformulation and analytical assessment

Curcumin was examined for colour, odour, physical form, melting point and solubility in selected media. Excess curcumin was added to each medium, maintained at 25 ± 2°C for 24 h with intermittent mixing, centrifuged and analysed after suitable dilution. The absorption maximum was determined by scanning a 10 µg/mL curcumin solution between 350 and 550 nm. Quantitative measurements were performed at 425.8 nm. A calibration curve was prepared using curcumin standard solutions in an ethanol–phosphate buffer pH 7.4 mixture (1:1), and linear regression was used for quantitative estimation.

Preliminary process and formulation screening

Mixing speed, sonication condition and sulfur hexafluoride-purging duration were evaluated during process standardisation. Formulation screening was then performed by varying Epikuron 200, chitosan and Pluronic F68 while maintaining curcumin at 10 mg, palmitic acid at 20 mg and the final volume at 10 mL. The batches were evaluated for particle size, PDI, entrapment efficiency and zeta potential.

Table 1: Preliminary formulation-screening batches and observed responses

Batch	Epikuron 200 (mg)	Chitosan (% w/v)	Pluronic F68 (% w/v)	Particle size (nm)	PDI	Entrapment efficiency (%)	Zeta potential (mV)
F1	60	0.20	0.25	472.07 ± 7.96	0.383 ± 0.002	55.67 ± 0.93	+22.40 ± 0.28
F2	80	0.20	0.25	427.47 ± 4.66	0.345 ± 0.005	63.47 ± 0.77	+23.84 ± 1.08
F3	120	0.20	0.25	363.97 ± 5.78	0.282 ± 0.005	74.08 ± 0.23	+26.23 ± 0.26
F4	160	0.20	0.25	426.67 ± 6.43	0.330 ± 0.005	77.08 ± 0.58	+27.22 ± 0.34
F5	120	0.05	0.25	347.37 ± 6.24	0.279 ± 0.010	66.18 ± 1.26	+18.42 ± 0.57
F6	120	0.30	0.25	433.17 ± 10.99	0.358 ± 0.005	76.96 ± 0.95	+32.20 ± 0.29
F7	120	0.20	0.05	445.40 ± 2.21	0.372 ± 0.007	70.44 ± 0.88	+28.88 ± 0.53
F8	120	0.20	0.40	340.13 ± 8.54	0.252 ± 0.007	76.30 ± 0.76	+22.70 ± 0.63
F9	120	0.20	0.50	331.10 ± 3.12	0.304 ± 0.012	73.79 ± 0.68	+20.48 ± 0.88

All batches contained curcumin 10 mg and palmitic acid 20 mg in a final volume of 10 mL. Values are mean ± SD, n = 3.

Preparation of the selected curcumin-loaded nanobubbles

Chitosan was dispersed in 1% v/v glacial acetic acid and stirred for 4–6 h. Pluronic F68 was dissolved separately in purified water and added to the chitosan phase. Curcumin, Epikuron 200 and palmitic acid

were dissolved in approximately 5 mL ethanol with gentle warming at 40–45°C. The ethanolic lipid phase was added gradually to the aqueous polymer-stabiliser phase under mechanical stirring at 1200 rpm for 15 min. Solvent evaporation was carried out at 40 ± 2°C for approximately 20 min. The dispersion was cooled and probe-sonicated in an ice bath at 30% amplitude using a 10 s ON/5 s OFF cycle for a total acoustic ON-time of 30 s. The final volume was adjusted to 10 mL, sulfur hexafluoride was purged through the dispersion for 60 s, and the formulation was transferred to tightly closed amber vials.

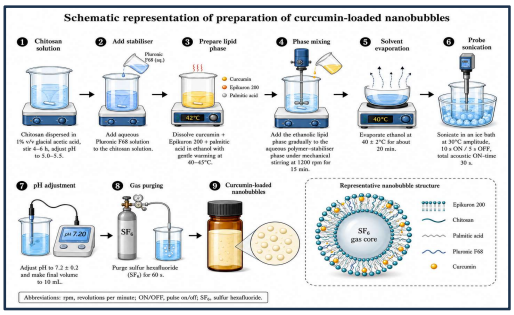

Figure 1: Schematic representation of the preparation of curcumin-loaded nanobubbles.

Table 2: Composition and processing conditions of the selected formulation

Component or condition	Selected value
Curcumin	10 mg
Epikuron 200	121 mg
Chitosan	0.22% w/v
Palmitic acid	20 mg
Pluronic F68	0.28% w/v
Final formulation volume	10 mL
Mixing speed and time	1200 rpm for 15 min
Probe sonication	30% amplitude; 10 s ON/5 s OFF; total acoustic ON-time 30 s
SF_6-purging duration	60 s

Physicochemical characterisation

Particle size and PDI were determined by dynamic light scattering after suitable dilution with filtered purified water. Zeta potential was measured using a folded-capillary cell at 25°C. Entrapment efficiency was determined indirectly by measuring unentrapped curcumin in the separated aqueous phase after centrifugation at 15,000 rpm for 30 min at 4°C. Drug loading was calculated from the mass of formulation-associated curcumin and the dried formulation-associated material.[7]

Morphological examination was performed by transmission electron microscopy for the blank and curcumin-loaded dispersions and by scanning electron microscopy for the dried selected formulation.

FTIR, DSC and PXRD studies

FTIR spectra of pure curcumin, the formulation components, the physical mixture and dried Cur-NBs were recorded over 4000–400 cm^{-1} and compared for retention, shifting, broadening or disappearance of characteristic bands.[8]

For DSC, approximately 3–8 mg of each sample was heated from 25 to 300°C at 10°C/min under nitrogen. PXRD patterns were recorded using Cu Kα radiation over a 2θ range of 5–50° and examined for changes in peak position, intensity and width.[9,10]

In vitro release study

Curcumin release was studied using a regenerated-cellulose dialysis membrane with a molecular-weight cut-off of 12,000–14,000 Da. A 2 mL formulation quantity equivalent to 2 mg curcumin was placed in the membrane and immersed in 100 mL phosphate-buffered saline containing 0.5% w/v Tween 80 at pH 7.4. The receptor medium was maintained at 37 ± 0.5°C and stirred at 100 rpm.[11,12]

For ultrasound-treated conditions, the formulation received one exposure at 1 MHz and 1.0 W/cm^2 for 30 s in pulsed mode with a 50% duty cycle before placement in the dialysis membrane. Samples were withdrawn at 0.5, 1, 2, 4, 6, 8, 12 and 24 h and replaced with fresh medium. Curcumin was quantified at 425 nm after addition of an equal volume of ethanol.

Release-kinetic analysis

The release profiles obtained at pH 7.4 with and without ultrasound were fitted separately to zero-order, first-order, Higuchi and Korsmeyer-Peppas models. The same eight non-zero sampling points (0.5, 1, 2, 4, 6, 8, 12 and 24 h) were used for every regression so that the numerical values in the kinetic table corresponded directly with all eight displayed graphs. Zero-order fitting was performed using cumulative percentage release versus time; first-order fitting used logarithm of percentage drug remaining versus time; Higuchi fitting used cumulative percentage release versus square root of time; and Korsmeyer-Peppas fitting used logarithm of fractional release versus logarithm of time. The full-profile Korsmeyer-Peppas fit was used for uniform comparison, and its mechanistic interpretation was therefore made cautiously because this model is conventionally interpreted using the earlier release region.[13]

RESULTS AND DISCUSSION

Preformulation findings

Curcumin was observed as a yellow-orange crystalline powder with a faint characteristic odour. The melting point was 181.65 ± 0.44°C. Solubility was extremely low in purified water (0.00058 ± 0.00004

mg/mL) and phosphate buffer pH 7.4 (0.00076 ± 0.00005 mg/mL), while addition of 0.5% Tween 80 increased the apparent solubility to 0.3747 ± 0.0125 mg/mL. The absorption maximum was observed at 425.8 nm. These findings supported the need for a carrier-assisted system and a surfactant-containing release medium. The calibration curve in ethanol–phosphate buffer pH 7.4 (1:1) showed good linearity, with the regression equation A = 0.0452C − 0.0059 and a coefficient of determination (R^2) of 0.9955.

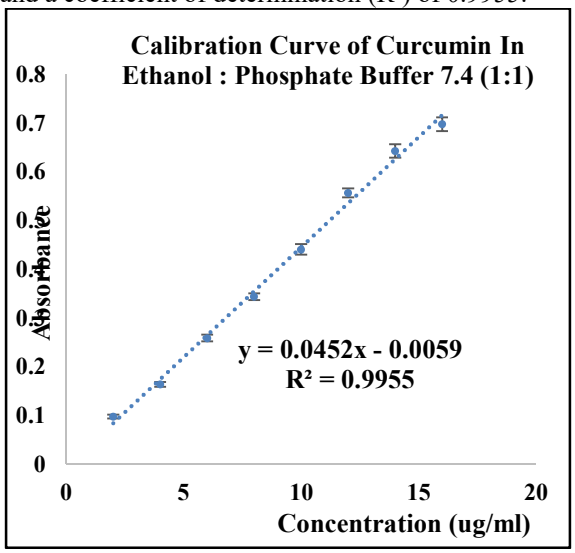

Figure 2: Calibration curve of curcumin in ethanol–phosphate buffer pH 7.4 (1:1) at 425.8 nm.

Effect of formulation variables and selection of composition

Increasing Epikuron 200 from 60 to 120 mg reduced particle size and increased entrapment efficiency, indicating improved interfacial coverage and a larger hydrophobic region for curcumin association. At 160 mg, entrapment remained high but the particle size increased, suggesting formation of larger phospholipid-associated structures. Increasing chitosan concentration raised zeta potential and entrapment efficiency, but the highest concentration also increased particle size and PDI, which may be related to increased viscosity and stronger association among hydrated polymer chains.

Pluronic F68 reduced particle size and PDI up to 0.40% w/v, consistent with improved steric stabilisation. At 0.50% w/v, particle size decreased further but PDI increased and positive zeta potential declined, indicating partial shielding of the chitosan-associated surface. The selected composition represented a balance among size, size distribution, drug association and positive surface charge rather than selection based on a single response.

Physicochemical properties of the selected formulation

Table 3: Physicochemical characteristics of the selected curcumin-loaded nanobubbles

Parameter	Observation or result
Appearance	Uniform opalescent dispersion
Colour	Pale yellow to yellow-orange
Visible coarse particles	Absent
Immediate phase separation	Not observed
Redispersibility	Readily redispersed after gentle mixing
pH	8.2 ± 0.2
Drug content	97.61 ± 0.49%
Mean particle size	361.8 ± 4.6 nm
PDI	0.286 ± 0.009
Zeta potential	+28.0 ± 0.7 mV
Entrapment efficiency	77.7 ± 0.9%
Drug loading	4.67 ± 0.03%

Values are mean ± SD, n = 3, for quantitative determinations.

The selected formulation showed a submicrometre mean size with a relatively narrow distribution. The positive zeta potential was consistent with surface contribution from chitosan and may assist electrostatic stabilisation. The high drug content and satisfactory entrapment efficiency indicated effective association of curcumin with the lipid-polymer matrix.

Morphological examination

Transmission electron microscopy showed rounded shell-containing structures in both blank and curcumin-loaded preparations. The curcumin-loaded carrier retained a distinct peripheral boundary with internal contrast. Scanning electron microscopy of the dried formulation showed rounded particulate structures with some clustering. Because drying may collapse gas-filled structures and increase apparent aggregation, the micrographs were interpreted as supportive morphological evidence rather than a direct measurement of the hydrated gas-core size.

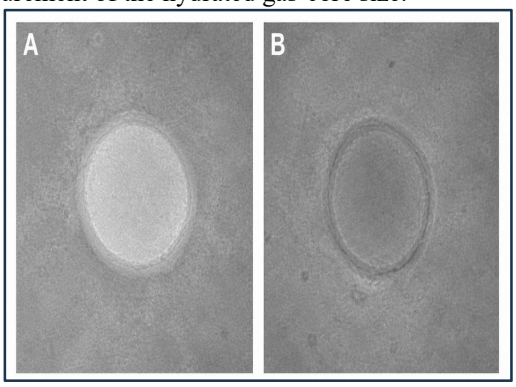

Figure 3: Transmission electron microscopy images of (A) unloaded and (B) curcumin-loaded chitosan nanobubbles.

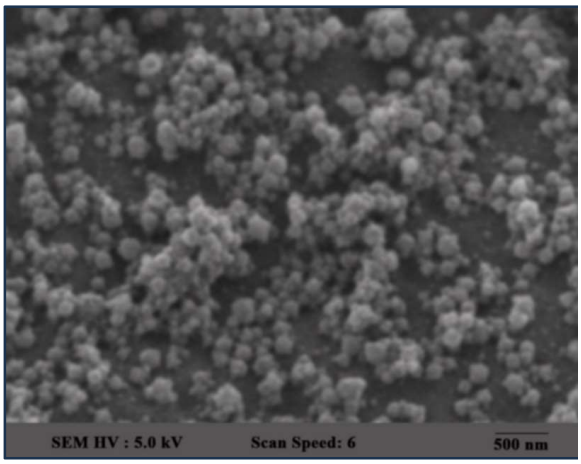

Figure 4: Scanning electron microscopy image of the dried selected curcumin-loaded nanobubble formulation.

FTIR compatibility assessment

Pure curcumin showed characteristic bands near 3508 cm^{-1} for phenolic O-H stretching, 1627 cm^{-1} for conjugated C=O stretching, 1602 cm^{-1} for aromatic C=C stretching, 1508 cm^{-1} for vibrations of the conjugated aromatic structure, 1276 cm^{-1} for aromatic C-O stretching, 1027 cm^{-1} for ether C-O-C vibrations and 812 cm^{-1} for aromatic C-H bending. The principal curcumin-associated bands remained identifiable in the physical mixture and dried Cur-NBs, although slight broadening and small shifts were observed. No prominent additional band or unexplained loss of the principal curcumin markers was detected, indicating absence of detectable chemical incompatibility and suggesting mainly non-covalent interactions within the formulation matrix.

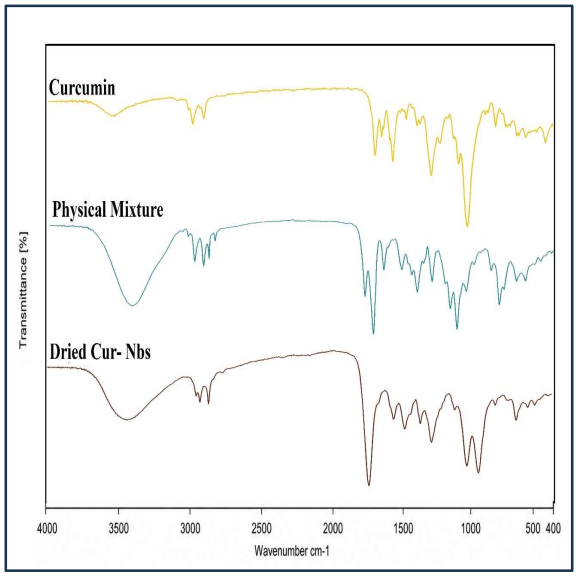

Figure 5: Comparative FTIR spectra of pure curcumin, physical mixture and dried selected curcumin-loaded nanobubbles.

Comparative DSC analysis

Pure curcumin showed a sharp endothermic peak near 178.6°C, confirming its crystalline nature. The physical mixture retained the curcumin-associated melting endotherm near 179.3°C, although with reduced intensity because of dilution by the excipients. In dried optimised Cur-NBs, the sharp curcumin melting endotherm was markedly weakened and broadened, with only a weak residual event near 176.4°C together with broader transitions arising from the formulation matrix. The comparative thermograms therefore supported reduction of curcumin crystallinity and finer dispersion of the drug within the nanobubble system rather than persistence of the drug in its original crystalline form.

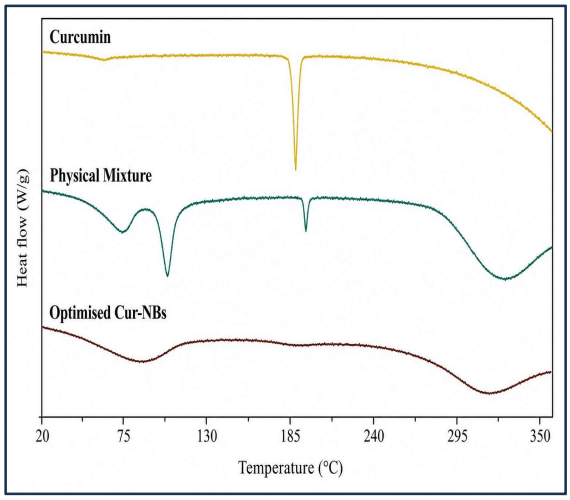

Figure 6: Comparative DSC thermograms of pure curcumin, physical mixture and dried optimised curcumin-loaded nanobubbles.

Comparative PXRD analysis

Pure curcumin showed multiple sharp and well-defined diffraction peaks, confirming its crystalline drug structure. The physical mixture retained several drug-associated reflections, demonstrating persistence of crystalline curcumin after simple mixing. In contrast, the dried optimised Cur-NBs showed marked reduction and broadening of the sharp drug peaks together with a broad diffuse halo extending mainly through 15–30° 2θ, indicating pronounced loss of long-range crystalline order after formulation. These PXRD findings agreed with the reduced and broadened curcumin melting behaviour observed during DSC analysis.

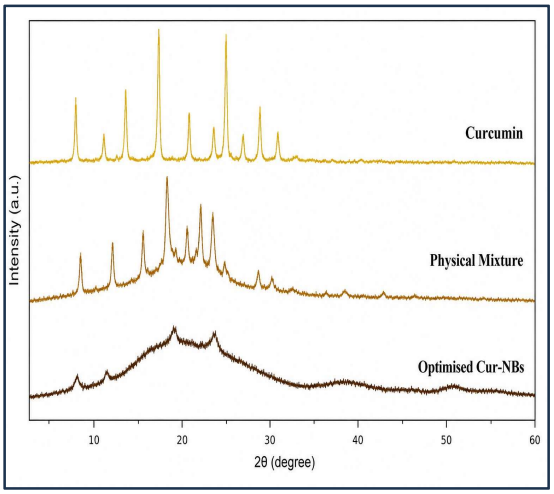

Figure 7: Comparative PXRD patterns of pure curcumin, physical mixture and dried optimised curcumin-loaded nanobubbles.

In vitro curcumin release

Table 4: Cumulative curcumin release at pH 7.4 with and without ultrasound

Time (h)	pH 7.4 without ultrasound (%)	pH 7.4 with ultrasound (%)
0	0.00 ± 0.00	0.00 ± 0.00
0.5	7.31 ± 0.80	17.81 ± 0.37
1	11.33 ± 0.96	27.51 ± 0.28
2	17.98 ± 0.83	39.09 ± 1.03
4	27.79 ± 0.41	50.54 ± 0.97
6	35.78 ± 0.45	60.79 ± 0.57
8	42.67 ± 0.77	68.30 ± 0.93
12	51.65 ± 0.84	76.40 ± 0.18
24	60.85 ± 0.54	83.56 ± 0.34

Values are mean ± SD, n = 3.

At pH 7.4 without ultrasound, cumulative curcumin release increased from 7.31 ± 0.80% at 0.5 h to 27.79 ± 0.41% at 4 h, 42.67 ± 0.77% at 8 h and 60.85 ± 0.54% at 24 h. The low initial release indicated that only a limited fraction of curcumin was immediately available in the external medium. The subsequent progressive increase suggested diffusion and desorption of the drug from the hydrated lipid-polymer shell rather than rapid loss of freely dispersed curcumin. The reduction in the apparent release rate during the later period was consistent with depletion of the readily releasable fraction and a longer diffusion path for drug remaining within the carrier-associated regions.

Ultrasound exposure increased curcumin release throughout the study. Cumulative release reached 17.81 ± 0.37% at 0.5 h, 50.54 ± 0.97% at 4 h, 68.30 ± 0.93% at 8 h and 83.56 ± 0.34% at 24 h. The ultrasound-associated increase was 10.50 percentage points at 0.5 h, 22.75 percentage points at 4 h and 25.63 percentage points at 8 h. This early and

intermediate enhancement may be related to oscillation of the gas-containing structures, temporary increase in shell permeability, partial disturbance of the lipid-polymer arrangement and reduction of the diffusional boundary surrounding the formulation.[14,15] The difference between the ultrasound and non-ultrasound profiles decreased from 25.63 percentage points at 8 h to 22.71 percentage points at 24 h. This narrowing did not indicate reversal of the ultrasound effect; rather, curcumin continued to diffuse from the untreated formulation during the later period, allowing the passive profile to approach the ultrasound-treated profile gradually. The absence of complete release at 24 h in either condition indicated that a residual fraction of curcumin remained associated with the carrier. Thus, the formulation displayed an ultrasound-responsive initial enhancement followed by continued sustained release from the remaining lipid-polymer structure.

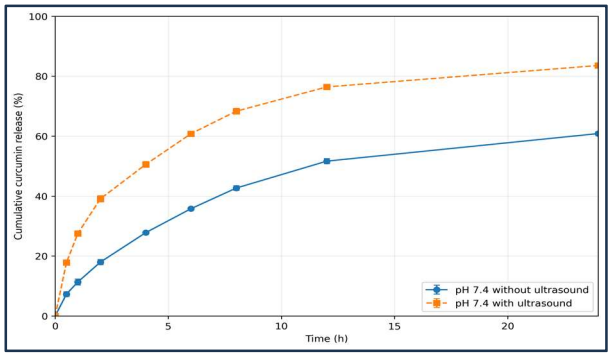

Figure 8: Comparative cumulative curcumin-release profiles of the selected formulation at pH 7.4 with and without ultrasound. Values are mean ± SD, n = 3.

Release kinetics

Table 5: Drug-release kinetic fitting at pH 7.4 with and without ultrasound

Release condition	Model	R^2	Kinetic constant	Unit	Release exponent, n
pH 7.4 without ultrasound	Zero order	0.8341	2.2500	% h^{-1}	—
	First order	0.9090	0.0371	h^{-1}	—
	Higuchi	0.9653	13.6304	% $h^{-1/2}$	—
	Korsmeyer-Peppas	0.9840	0.1176	h^{-n}	0.577
pH 7.4 with ultrasound	Zero order	0.7352	2.5764	% h^{-1}	—
	First order	0.8905	0.0678	h^{-1}	—
	Higuchi	0.9127	16.1640	% $h^{-1/2}$	—
	Korsmeyer-Peppas	0.9654	0.2715	h^{-n}	0.409

All four kinetic models were fitted using the same eight non-zero sampling points under both release conditions. Consequently, each kinetic graph contains eight observed points, and the regression equations, kinetic constants and R^2 values shown in the graphs correspond directly with Table 5.

Zero-order model

The zero-order model produced R^2 values of 0.8341 without ultrasound and 0.7352 with ultrasound. These were the lowest values among the four models, showing that curcumin was not released at a constant rate over the complete 24 h period. The non-zero intercepts and visible deviation of the later points from the regression lines reflected the presence of an initial readily releasable fraction followed by a progressively slower phase. The lower R^2 after ultrasound was expected because a single acoustic exposure produced a pronounced early increase that could not be represented adequately by one constant-rate line. Therefore, the formulation did not display ideal zero-order release under either condition.

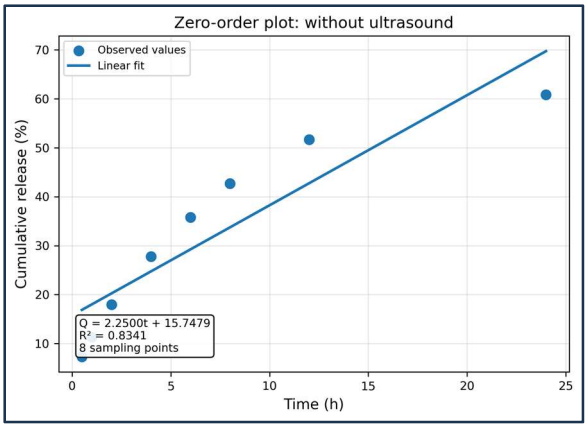

Figure 8A: Zero-order release plot at pH 7.4 without ultrasound (eight sampling points).

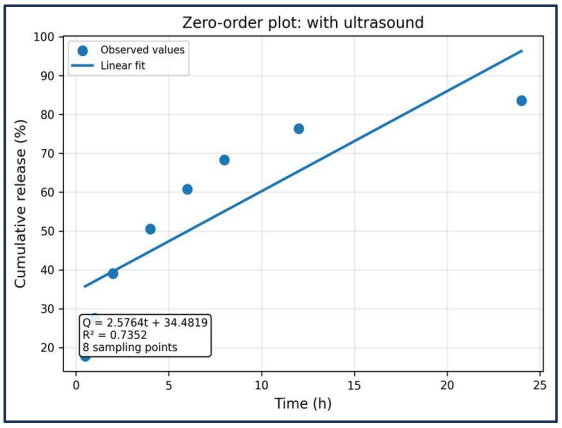

Figure 8B: Zero-order release plot at pH 7.4 with ultrasound (eight sampling points).

First-order model

First-order fitting improved the R^2 values to 0.9090 without ultrasound and 0.8905 with ultrasound. The better fit than the zero-order model indicated that the release rate was influenced by the quantity of curcumin remaining in the formulation. The first-order constant increased from 0.0371 h^{-1} without ultrasound to 0.0678 h^{-1} after ultrasound exposure, representing an approximately 1.83-fold increase. This change was consistent with greater drug availability after acoustic perturbation of the carrier. Nevertheless, the first-order model did not provide the highest R^2, indicating that concentration-dependent release alone could not explain the complete profile.

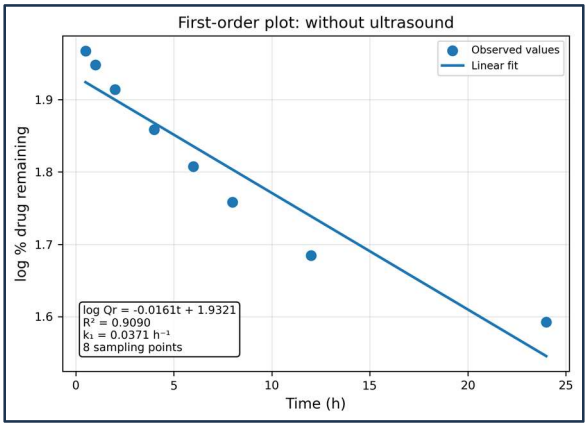

Figure 8C: First-order release plot at pH 7.4 without ultrasound (eight sampling points).

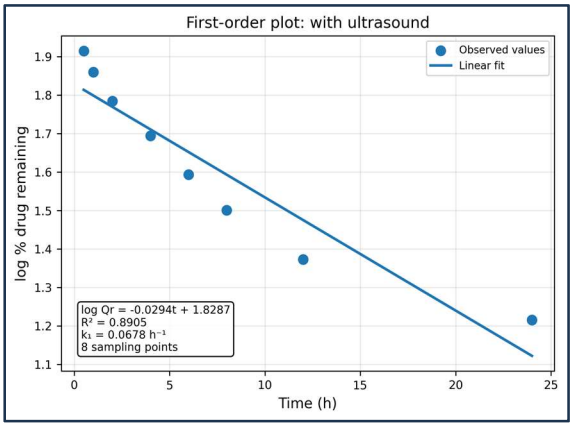

Figure 8D: First-order release plot at pH 7.4 with ultrasound (eight sampling points).

Higuchi model

The Higuchi model showed strong linearity, with R^2 values of 0.9653 without ultrasound and 0.9127 with ultrasound. The Higuchi constant increased from 13.6304 to 16.1640% $h^{-1/2}$ after ultrasound, corresponding to an increase of about 18.6%. The comparatively high R^2 values supported an important contribution from diffusion through the hydrated shell and carrier-associated regions. The lower fit after ultrasound indicated that the acoustically triggered initial mobilisation of curcumin introduced an additional process beyond simple square-root-of-time diffusion. The Higuchi interpretation was considered supportive rather than definitive because the nanobubble system is structurally different from an ideal homogeneous planar matrix.

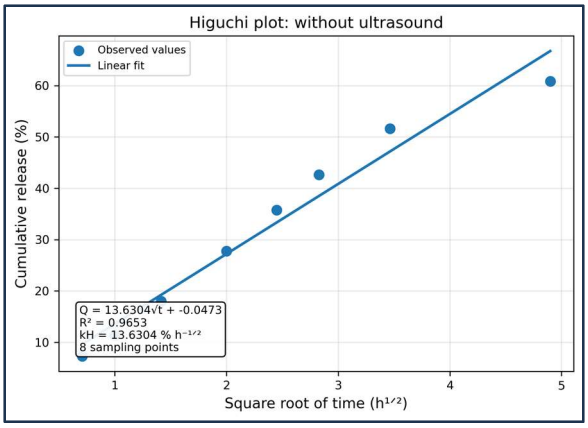

Figure 8E: Higuchi release plot at pH 7.4 without ultrasound (eight sampling points).

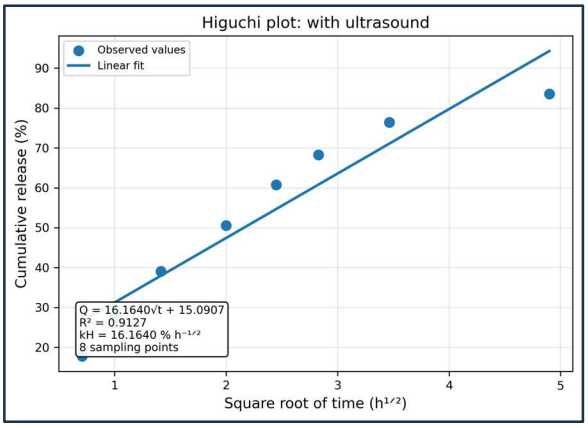

Figure 8F: Higuchi release plot at pH 7.4 with ultrasound (eight sampling points).

Korsmeyer-Peppas model

The Korsmeyer-Peppas model provided the highest R^2 under both conditions: 0.9840 without ultrasound and 0.9654 with ultrasound. The release constant increased from 0.1176 to 0.2715 h^{-n} after acoustic exposure, representing an approximately 2.31-fold increase and confirming the greater release rate observed experimentally. The release exponent was 0.577 without ultrasound, indicating a combined contribution from diffusion and relaxation or reorganisation of the hydrated lipid-polymer structure. After ultrasound, the exponent decreased to 0.409, which was close to the range associated with diffusion-dominated release from approximately spherical carriers. This reduction suggested that acoustic exposure increased permeability and shortened the effective diffusion pathway, making post-exposure drug movement more strongly controlled by diffusion.[13]

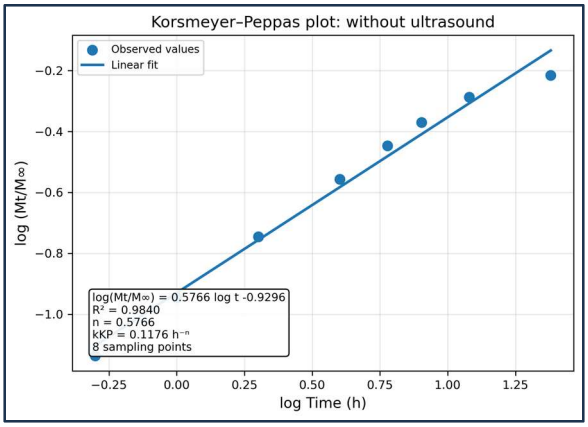

Figure 8G: Korsmeyer-Peppas release plot at pH 7.4 without ultrasound (eight sampling points).

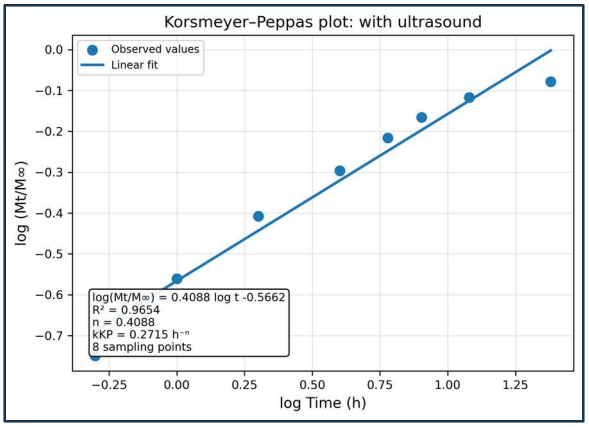

Figure 8H: Korsmeyer-Peppas release plot at pH 7.4 with ultrasound (eight sampling points).

Comparative interpretation of release kinetics

For the non-ultrasound profile, the model-fit order was Korsmeyer-Peppas (R^2 = 0.9840) > Higuchi (0.9653) > first order (0.9090) > zero order (0.8341). The same order was obtained after ultrasound: Korsmeyer-Peppas (0.9654) > Higuchi (0.9127) > first order (0.8905) > zero order (0.7352). The consistently stronger performance of the Korsmeyer-Peppas and Higuchi models indicated that diffusion was a major contributor, while the change in the release exponent suggested that structural hydration and relaxation contributed more strongly before acoustic exposure. Ultrasound increased every calculated release constant, but it reduced the R^2 of each simple model because the treated profile combined two distinguishable phases: a rapid acoustically stimulated release followed by slower diffusion from residual carrier-associated material. The models therefore described the observed profiles but did not establish a single exclusive release mechanism.

CONCLUSION

Curcumin-loaded nanobubbles were successfully formulated using Epikuron 200, chitosan, palmitic

acid and Pluronic F68 with sulfur hexafluoride as the gaseous phase. Preliminary formulation screening demonstrated that the phospholipid, polymer and stabiliser concentrations influenced particle size, distribution width, drug entrapment and surface charge. The selected formulation showed satisfactory particle size, PDI, positive zeta potential, entrapment efficiency and drug loading. FTIR indicated compatibility of curcumin with the formulation components, while comparative DSC and PXRD demonstrated reduced crystalline order after incorporation into the carrier matrix. At pH 7.4, ultrasound increased cumulative release from 60.85 ± 0.54% to 83.56 ± 0.34% at 24 h. Eight individual kinetic graphs, each containing the same eight sampling points, showed that the Korsmeyer-Peppas model provided the best descriptive fit under both conditions. Ultrasound increased the release constants and shifted the profile towards a stronger diffusion-dominated contribution. These findings support the developed nanobubbles as a suitable ultrasound-responsive formulation platform for subsequent biological and therapeutic evaluation.

FUTURE DIRECTIONS

Further work should establish the long-term physical and chemical stability of the formulation, including changes in particle size, PDI, zeta potential, curcumin content, gas retention and redispersibility under defined storage conditions. The effects of sterilisation, container-closure selection, scale-up and batch-to-batch reproducibility should also be examined before translation to larger studies. Ultrasound parameters such as frequency, intensity, pulse duration and duty cycle require systematic optimisation to identify conditions that provide reproducible release without excessive heating or structural damage. Subsequent biological evaluation should include cellular uptake, cytotoxicity, apoptosis and selectivity studies in appropriate breast-cancer and non-cancerous cell models, followed by pharmacokinetic, biodistribution, safety and antitumour studies in suitable in vivo models. These investigations would clarify whether the physicochemical and ultrasound-responsive advantages observed in vitro can be translated into improved therapeutic exposure and tumour-directed performance.

ACKNOWLEDGEMENT

The authors acknowledge HSBPVT's GOI Faculty of Pharmacy, Kashti, for providing laboratory support and acknowledge the instrumentation facilities used for FTIR, DSC, PXRD and electron-microscopy studies.

ETHICAL APPROVAL

Not applicable. The work reported in this manuscript did not involve human participants, experimental animals or cell-line experiments.

CONFLICT OF INTEREST

The authors declare that there is no conflict of interest related to this work.

FUNDING

No external funding was received for the work reported in this manuscript.

DATA AVAILABILITY

The numerical data supporting the findings are included within the manuscript. Additional raw instrumental data may be made available by the corresponding author upon reasonable request.

REFERENCES

1. Sharifi-Rad J, Rayess YE, Rizk AA, et al. Turmeric and its major compound curcumin on health: bioactive effects and safety profiles for food, pharmaceutical, biotechnological and medicinal applications. Front Pharmacol. 2020;11:1021.
2. Patel SS, Acharya A, Ray RS, et al. Cellular and molecular mechanisms of curcumin in prevention and treatment of disease. Crit Rev Food Sci Nutr. 2020;60:887-939.
3. Xiong R, Xu RX, Huang C, et al. Stimuli-responsive nanobubbles for biomedical applications. Chem Soc Rev. 2021;50:5746-5776.
4. Hernot S, Klibanov AL. Microbubbles in ultrasound-triggered drug and gene delivery. Adv Drug Deliv Rev. 2008;60:1153-1166.
5. Jayasankar G, Koilpillai J, Narayanasamy D. A systematic study on long-acting nanobubbles: current advancement and prospects on theranostic properties. Adv Pharm Bull. 2024;14:278-301.
6. Elbana E, Elzayat AM, Abdelrazek EM, et al. Synthesis and characterization of chitosan based micro/nanobubbles for potential biomedical applications. J Inorg Organomet Polym Mater. 2025;35:9290-9303.
7. Joudeh N, Linke D. Nanoparticle classification, physicochemical properties, characterization, and applications: a comprehensive review for biologists. J Nanobiotechnology. 2022;20:262.
8. Bunaciu AA, Aboul-Enein HY, Fleschin S. Application of Fourier transform infrared spectrophotometry in pharmaceutical drugs analysis. Appl Spectrosc Rev. 2010;45:206-219.
9. Stankovic M, Frijlink HW, Hinrichs WLJ. Polymeric formulations for drug release prepared by hot melt extrusion: application and characterization. Drug Discov Today. 2015;20:812-823.
10. Rodriguez I, Singh RG, Tinoco AD. Using X-ray diffraction techniques for biomimetic drug development, formulation, and polymorphic characterization. Biomimetics (Basel). 2020;6:1.
11. Weng J, Tong HHY, Chow SF. In vitro release study of the polymeric drug nanoparticles:

development and validation of a novel method. Pharmaceutics. 2020;12:732.
12. Jug M, Hafner A, Lovric J, et al. In vitro dissolution/release methods for mucosal delivery systems. ADMET DMPK. 2017;5:173.
13. Wu IY, Bala S, Skalko-Basnet N, et al. Interpreting non-linear drug diffusion data: utilizing Korsmeyer-Peppas model to study drug release from liposomes. Eur J Pharm Sci. 2019;138:105026.
14. Rapoport N, Kennedy A, Shea J, et al. Controlled and targeted tumor chemotherapy by ultrasound-activated nanoemulsions/microbubbles. J Control Release. 2009;138:268-276.
15. Radha R, Paul V, Anjum S, et al. Enhancing curcumin therapeutic potential in cancer treatment through ultrasound-mediated liposomal delivery. Sci Rep. 2024;14:10499.